



UNIVERSITY
OF WOLLONGONG
AUSTRALIA

University of Wollongong
Research Online

Faculty of Engineering - Papers (Archive)

Faculty of Engineering and Information Sciences

2006

In-situ observation of sulfide precipitation in a low-carbon, titanium alloyed steel

Sima Aminorroaya-Yamini

University of Wollongong, sima@uow.edu.au

Rian J. Dippenaar

University of Wollongong, rian@uow.edu.au

Mark H. Reid

University of Wollongong, mreid@uow.edu.au

<http://ro.uow.edu.au/engpapers/947>

Publication Details

Aminorroaya-Yamini, S., Dippenaar, R. J. & Reid, M. H. (2006). In-situ observation of sulfide precipitation in a low-carbon, titanium alloyed steel. In M. Baker (Eds.), *Proceedings of the Iron and Steel Technology Conference (AISTech 2006)* (pp. 319-326). Warrendale, USA: The Association of Iron and Steel Technology.

Research Online is the open access institutional repository for the University of Wollongong. For further information contact the UOW Library:
research-pubs@uow.edu.au

In-situ Observation of Sulfide Precipitation in a Low-carbon, Titanium Alloyed Steel

Sima Aminorroaya
Faculty of Engineering, University of Wollongong
Northfield Ave., Wollongong
NSW 2522, Australia
Tel: +61-2-42215718
Fax: +61-2-4221 3662
E-mail: say981@uow.edu.au

Rian Dippenaar
Tel: +61-2-42214498
Fax: +61-2-4221 3662
E-mail: rian@uow.edu.au

Mark Reid
Tel: +61-2-42214859
Fax: +61-2-4221 3662
E-mail: mark@uow.edu.au

Key words: Sulfide precipitates, low carbon, low manganese, titanium, Laser-scanning confocal microscope

INTRODUCTION

Removal of inclusions is of great significance to steelmakers and the scientific principles underpinning inclusion removal has been the subject of numerous investigations in the past and during the last few decades, it has become increasingly obvious that inclusions can be utilized as an effective tool for the control of microstructure¹. Manganese sulfide precipitates are known to crystallize and precipitate preferentially in interdendritic regions during solidification, due to segregation of manganese and sulphur² and these inclusions have traditionally been used for the dual purpose of improving the machinability and controlling of grain structure in steel. Small MnS particles restrain grain growth in steel and Wakoh et al.³ have shown that deoxidation practice can be used as a means to control the size and distribution of MnS. Moreover, microstructural control by manipulating the precipitation of sulfides has been used extensively to improve the toughness of microalloyed steels in general and specifically the toughness of heat-affected zones in welds³.

During hot rolling, manganese sulfide inclusions, which are plastic at elevated temperatures, become highly elongated in the rolling direction. These MnS-stringered inclusions drastically reduce the formability of steel and specifically have an influence on ductility, stretchability and the critical strain at the onset of failure. The deleterious effect of such inclusions on formability can be minimized or even eliminated by sulfide shape control⁴.

The morphology and formation of the MnS phase has been classified by Kiessling in four different categories as follows⁵: randomly distributed drop like (Type I), rod like (Type II), mono phase equiaxed precipitates (Type III) and crystallized plate like sulfides (Type IV). Oikawa et al.⁶ proposed that primary MnS inclusions can be classified as follows: i) spherical (formed while both the matrix and MnS phase are liquid), ii) dendritic (formed by primary crystallization in a highly supersaturated liquid), iii) angular morphologies (formed by primary crystallization under a low degree of supersaturation). However, secondary MnS inclusions are classified as follows: i) monotectic (formed through the metastable monotectic reaction), ii) rod-like eutectic, iii) irregular eutectic (formed through the non-cooperative eutectic reaction). These specific morphologies being a function of the nature of the oxides and nitrides that act as nucleants for the MnS inclusion formation⁷.

Sulfide inclusions of the MnS-type in alloyed steels may have different amounts of alloying elements in solid solution with a concomitant increase in hardness of the inclusion without the optical appearance of the inclusion in the microscope being affected⁵. Titanium is one of the most potent elements that can change the composition and mechanical properties of manganese sulfide inclusions.

Earlier studies^{1, 6, 8} of MnS precipitation in low carbon, high manganese titanium added steels have shown that manganese sulfides are dominant while titanium additions decrease the average size of manganese sulfides but leads to an increase in the density of precipitates in Ti killed steel as a result of liquid nuclei of (Ti,Mn)O acting as heterogeneous nucleation sites for the precipitation of MnS¹. On the other hand, studies^{3, 9-13} which evaluated the precipitation in ultra low carbon, low manganese titanium alloyed steels, have shown that TiS and Ti₄C₂S₂ precipitate preferentially. It is not clear at present to what extent carbon content and titanium additions influence manganese sulfide composition, morphology and sequence of precipitation. For instance, Iorio et al.¹⁴ maintain that TiS should not be present when the C content exceeds 0.02%. This implies that Ti₄C₂S₂ would be preferred to TiS. Hence, steel composition and specifically manganese content seem to have a dominant influence and further studies are required to investigate the nature, morphology and composition of sulfide precipitates in low carbon, low manganese, and titanium added steel.

Laser-scanning confocal microscope (LSCM) in combination with an infrared image furnace has been used to observe the dynamic crystal growth in an Fe-C alloy directly for the first time by Shibata et al.¹⁵. With this instrument, it has also been possible to observe in-situ, the precipitation of MnS at high temperature¹⁶. Various attempts have been made in the past^{2, 7, 17} to observe MnS formation on the surface of steels during microsegregation. On the other hand, macrosegregation, which occurs over large distances due to the physical movement of liquid or solid phases has not received the same attention in the literature¹⁸.

In the current study, a newly developed concentric solidification technique¹⁹ has been employed to observe in-situ solidification and precipitation during segregation in steels with low carbon, manganese, and sulfur contents to which small additions of titanium has deliberately been made. By using this experimental technique, it has been possible to observe macrosegregation and to simulate alloying element segregation during continuous casting of steel. It has been possible to observe the solidification of the highly segregated liquid and the precipitation of the components with the lowest melting points in the inter-dendritic regions.

EXPERIMENTS

The bulk chemical composition of the steel that was studied is shown in table I. Previous studies⁴ concerned with inclusions in low carbon, low manganese steels have indicated the presence of oxide inclusions, mostly alumina, and MnS stringers and we have chosen the composition shown in the table to enable us to examine the effect of titanium on the morphology, composition and occurrence of sulfide precipitates.

Table I: Bulk chemical composition of steel (percentage by mass)

Element	C	Mn	S	Al	Ti
Percent	0.1	0.3	0.01	0.03	0.024

Figure 1 shows a schematic of the laser-scanning confocal microscope chamber and sample holder, which was used to conduct the in-situ observation of sulfide precipitation. The principle and method of operation have been described in detail elsewhere¹⁹. In the concentric solidification experimental technique, a centralized pool of liquid metal is contained by a rim of solid of the same material under a radial thermal gradient in a specimen that is typically 10 mm in diameter and 400 μm thick. A schematic diagram of a liquid pool contained by a solid rim in such an arrangement is shown in Figure 2.

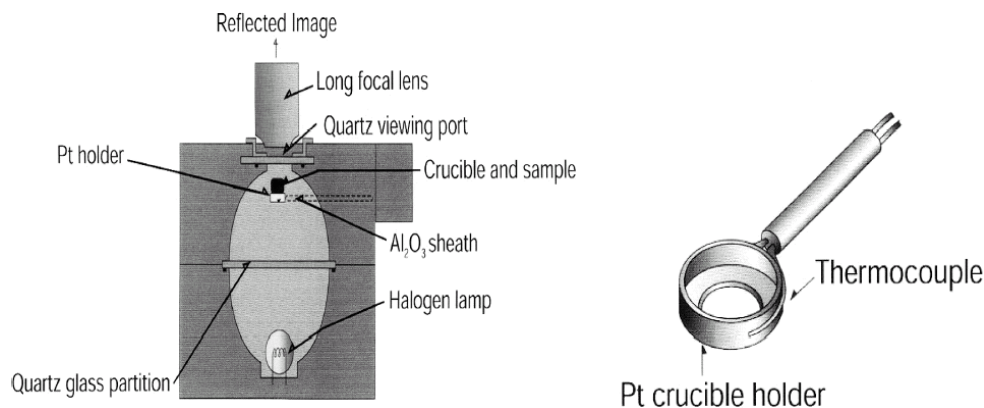


Figure 1: Schematic of laser-scanning confocal microscope chamber and sample holder

A small piece of steel is machined into a disc (10 mm diameter, 0.4 mm thick); mirror polished on both sides; placed in an alumina crucible (10 mm diameter and 2 mm height) and heated at the rate of 100°C/min under ultra high purity argon gas. Because the sample is positioned in the furnace chamber at one focal point of the ellipsoidal cavity and the heating element at the other focal point, the radiative heat source is concentrated in the center of the disc-shaped specimen and a sharp radial temperature gradient develops in the specimen¹⁹. The center of the sample is melted; heated to approximately 1600°C and kept at this temperature for 6 minutes. This procedure ensures that a stable melt pool is formed with a solid rim surrounding the liquid pool. The specimen is then cooled to 1100°C at a rate of 20°C/min followed by cooling to room temperature at a rate of 100°C/min.

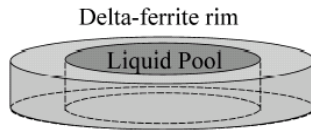


Figure 2: Schematic diagram of concentric solidification

The surface image of the sample is continuously recorded. Once a stable liquid pool has formed solidification initiates on cooling from the solid rim of delta-ferrite and the liquid, with its continuously changing composition and enrichment in alloying elements, remains in the center of disc until the final stages of solidification. Following the observation in the confocal microscope, the specimen was transferred to a scanning electron microscope (SEM) equipped with energy dispersive spectroscopy (EDS) to analyze the components that were formed during solidification and were visible on the surface of the specimen that was observed in the confocal microscope. Specimens were subsequently sectioned and cross sections subjected to SEM analysis.

RESULTS AND DISCUSSION

During heating, some small particles were floating on the surface of the liquid as shown in Figure 3. These particles are most probably original inclusions that floated out or are the result of reaction between liquid steel and the crucible or furnace atmosphere but they disappeared after a few minutes, driven by Marangoni forces out of the field of view towards the solid rim.



Figure 3: Floating particles on the surface of liquid steel during heating

During cooling, the solidification of δ -ferrite proceeds from the solid rim towards the center of the disc-shaped sample. On occasion, some dendrites formed ahead of the advancing liquid/solid interface within the molten pool as shown in Figure 4.

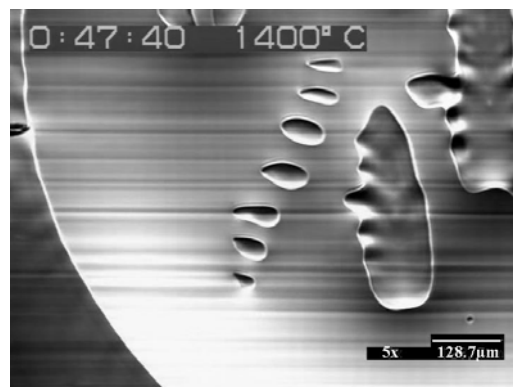


Figure 4: δ -ferrite dendrites that formed in the molten pool

Following solidification at the liquid/solid interface, δ -ferrite transforms to austenite and the remaining liquid, enriched in alloying elements finally solidifies in the center of the disc. Although impossible to observe, the remaining liquid is specifically enriched in carbon and the final liquid that solidifies will have a carbon concentration significantly higher than the bulk specimen. This is of course, exactly what happens during continuous casting of steel.

In the final stages of solidification, a group of small particles suddenly appears on the surface of the sample and grows very fast to cover most the surface of the remaining liquid as shown in Figure 5. Following the observation of the formation of these particles in the confocal microscope, the sample was transferred for observation in the scanning-electron microscope. Figure 6 shows a typical SEM micrograph of precipitates that formed during solidification in the segregated area. EDS analysis of similar precipitates indicates the presence of titanium and sulfur within the particles while the manganese content is very low as shown in Figure 7. It is not possible to determine quantitatively the carbon distribution using EDS analysis and hence, it is not possible to distinguish between TiS and $Ti_4C_2S_2$. This is the subject of further studies.

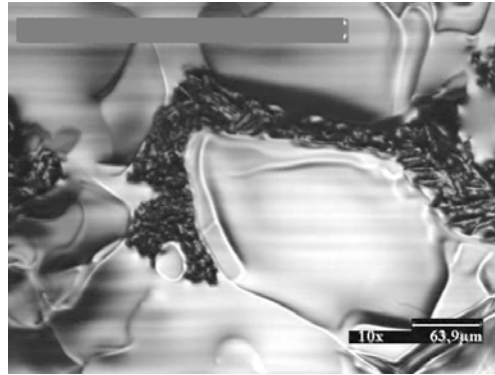


Figure 5: In-situ observation of sulfide precipitation on the surface of the LSCM sample

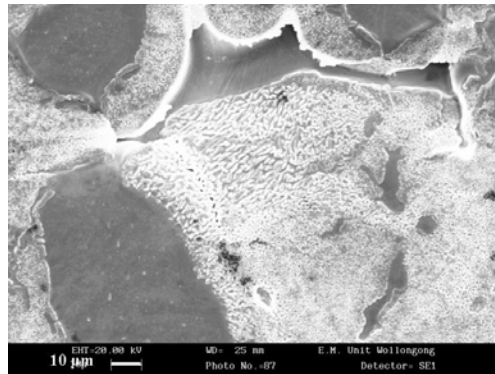


Figure 6: SEM photograph of a colony of precipitates

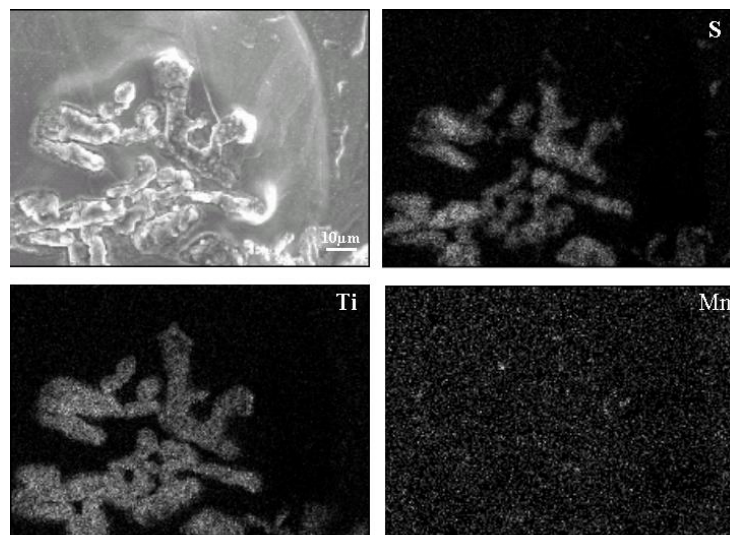


Figure 7: X-ray mapping of precipitates

The rod-like morphology of the precipitates would suggest that they may have formed by an eutectic reaction but the LSCM observations did not provide any evidence of the occurrence of such a reaction. The binary phase diagram Fe-TiS has not been determined yet, but a schematic representation of a likely phase diagram is shown in Figure 8²⁰. If it is assumed that the chemical composition of the segregated liquid is that of the dotted line in the figure, it follows that on cooling from the liquid state, primary titanium sulfide particles (TiS) will form followed by the transformation ($L_1 \rightarrow L_1 + \text{Fe}(s) + \text{TiS}(s)$). Should it be assumed that this transition will occur, it is possible that the precipitates nucleate heterogeneously on the solid rim at the progressing solid/liquid interface. Although solid iron, that may form through such a transformation can not be distinguished in the SEM, the sudden appearance of a bright phase was observed on the surface of the sample in the confocal microscope, associated with titanium sulfide particles as shown in Figure 9. This bright phase might well be solid iron. A cross section of a sample observed in the scanning electron microscope is shown in Figure 10; the morphology of this group of precipitates is similar to rod like eutectic sulfides according to the classification of Oikawa et al.⁶.

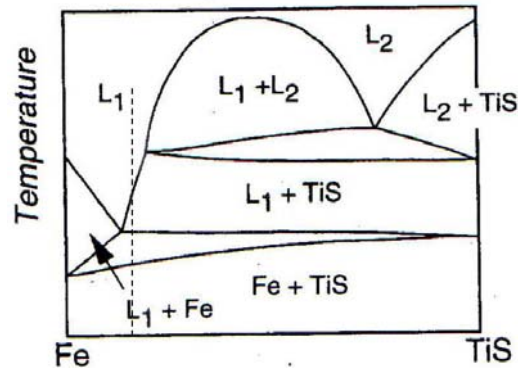


Figure 8: Schematic phase diagram of TiS pseudo-binary system²⁰

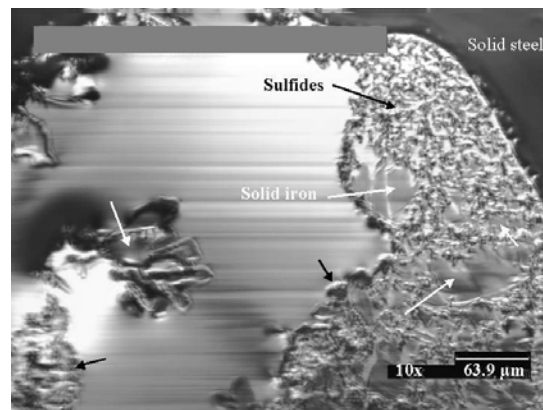


Figure 9: Presence of liquid steel as well as two different phase of solid at the LSCM sample

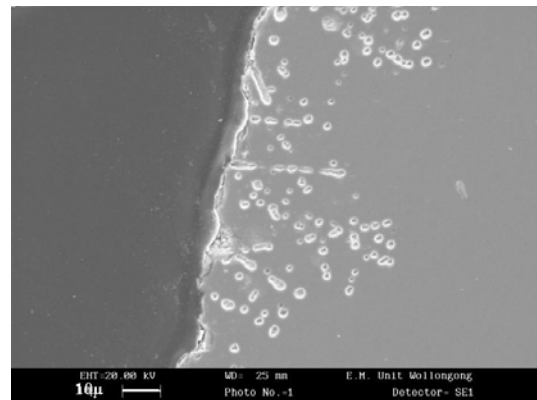


Figure 10: The morphology of sulfide precipitates in a cross section of the disc-shaped specimen

If it is assumed that the solidification path of the liquid in the center of the specimen is that shown in Figure 8, primary (solid) titanium sulfide will form according to reaction (1):



The solubility product of this reaction has been reported in literature¹² as:

$$\log[\text{Ti}][\text{S}] = -13975/T + 5.43 \quad (2)$$

Hence, the likelihood of titanium sulfide precipitation can be calculated as a function of temperature as shown in Figure 11. The horizontal line in this figure is the solubility product $[\text{Ti}][\text{S}]$ based on the bulk composition of the steel shown in Table 1. Consequently, precipitation of TiS is not possible in liquid steel until significant segregation of titanium and sulfur has occurred during solidification.

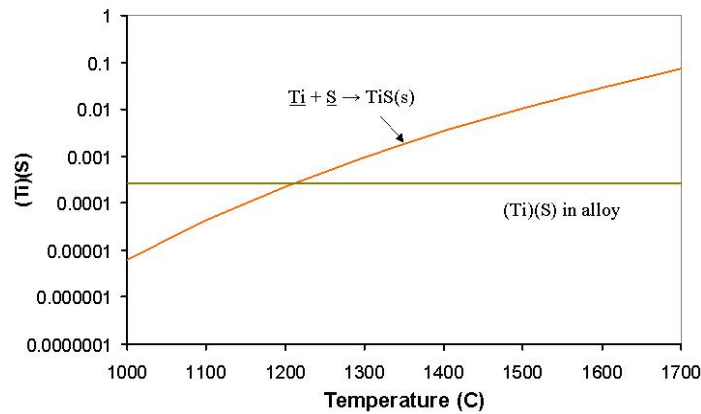


Figure 11: Solubility product $[\text{Ti}][\text{S}]$ for $(\text{TiS})_s$ precipitation as a function of temperature

Another group of precipitates appeared in the austenite phase during cooling. Figure 12(a) shows these precipitates captured by LSCM and Fig. 12(b) is a typical SEM observation of the precipitates shown in photo 12(a). The precipitates are less than $3\mu\text{m}$ in size with an angular or rod-like shape. EDS analysis indicates the presence of Mn, Ti, and particularly sulfur in these particles. Kimura et al.¹⁷ argued that diffusion of elements in the solid state leads to the formation of this group of precipitates and it is likely that Fe may also be contained in the lattice of these particles although the presence of iron within these particles cannot be detected by EDS analysis.

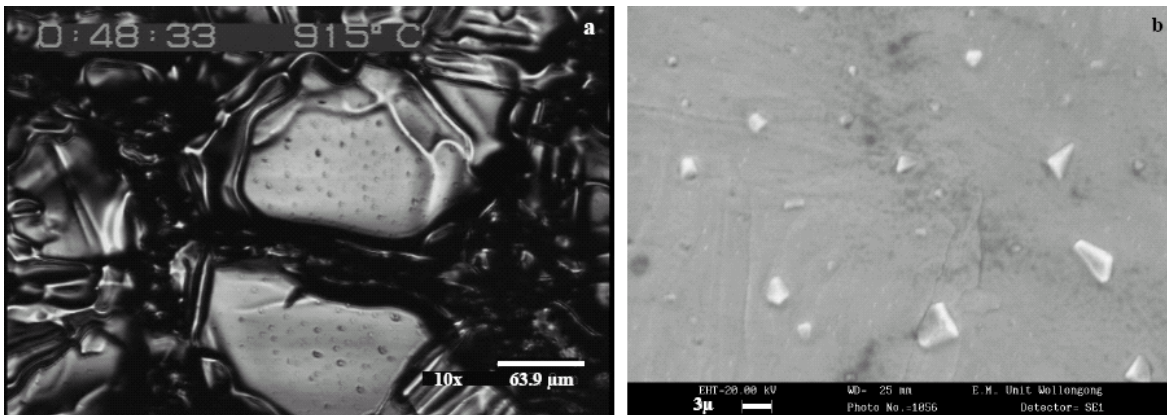


Figure 12: a) LSCM image of sulphide particles appearing within austenite grains b) SEM observation of the same particles

CONCLUSIONS

- A concentric solidification technique has been used to simulate segregation and the concomitant precipitation of sulphides during the continuous casting of steel.

- Observations in a laser-scanning confocal microscope in conjunction with an infra-red heating furnace, revealed important aspects of sulfide precipitation morphology and the composition of sulfides that form in a low carbon, low manganese steel containing titanium.
- Primary TiS (and/or Ti₄C₂S₂) precipitates, containing very little or no manganese, precipitate from the liquid on cooling.
- Once the steel has completely solidified, (Mn,Ti)S, possibly also containing Fe in the lattice, precipitates from austenite.
- It seems that most of the titanium is consumed during the formation of primary sulfides and only when the solubility of sulfur decreases on solidification, does the formation of Mn,Ti)S become thermodynamically attractive.

ACKNOWLEDGEMENT

We should like to thank the University of Wollongong for permission to publish this work and BlueScope Steel for supporting the project.

REFERENCES

1. K. Oikawa, K. Ishida, and T. Nishizawa, "Effect of titanium addition on the formation and distribution of MnS inclusions in steel during solidification", *ISIJ International (Japan)*, Vol. 37, No. 4, 1997, pp. 332-338.
2. M. Valdez, Y. Wang, and S. Sridhar, "MnS precipitation behavior in Re-sulfurized steels with intermediate levels of sulfur", *steel research international*, Vol. 76, 2005, pp. 306-312.
3. N. Tsunekage, and H. Tsubakino, "Effects of Sulfur Content and Sulfide-forming Elements Addition on Impact Properties of Ferrite–Pearlitic Microalloyed Steels", *ISIJ international*, Vol. 41, 2001, pp. 498-505.
4. S.K. Paul, and A. Ray, "Influence of inclusion characteristics on the formability and toughness properties of a hot-rolled deep-drawing quality steel", *Journal of Materials Engineering and Performance (USA)*, Vol. 6, No. 1, 1997, pp. 27-34.
5. R. Kiessling, and N. Lange, *Non-Metallic Inclusions in Steel*. second ed. 1997: The institute of materials.
6. K. Oikawa, H. Ohtani, K. Ishida, and T. Nishizawa, "The control of the morphology of MnS inclusions in steel during solidification", *ISIJ Int. (Japan)*, Vol. 35, 1995, pp. 402-408.
7. M.E. Valdez, Y. Wang, and S. Sridhar, "In-Situ Observation of the Formation of MnS during Solidification of High Sulphur Steels", *Steel Research International*, Vol. 75, 2004, pp. 247-256.
8. K. Oikawa, Y. Ohuchi, and K. Ishida. *Effect of Ti and Al addition on the distribution of MnS inclusion in steel during solidification*. in *THERMEC 97: International Conference on Thermomechanical Processing of Steels and Other Materials*. 1997. Wollongong; Australia; 7-11 July 1997.
9. M. Hua, G.K. Eloit, and A.J. DeArdo, "Identification of Ti-S-C containing multi-phase precipitates in ultra-low carbon steels by analytical electron microscopy", *ISIJ International*, Vol. 37, 1997, pp. 1129-1132.
10. M. Hua, C.I. Garcia, and A.J. DeArdo, "Precipitation behavior in ultra-low-carbon steels containing titanium and niobium", *Metallurgical and Materials Transactions A*, Vol. 28A, 1997, pp. 1769-1780.
11. N. Yoshinaga, K. Ushioda, S. Akamatsu, and O. Akisue, "Precipitation Behavior of Sulfides in Ti-added Ultra Low-carbon Steels in Austenite", *ISIJ Int.*, Vol. 34, 1994, pp. 24-32.
12. X. Yang, D. Vanderschueren, J. Dilewijns, C. Standaert, and Y. Houbaert, "Solubility Products of Titanium Sulphide and Carbosulphide in Ultra-low Carbon Steels", *ISIJ international*, Vol. 36, 1996, pp. 1286-1294.
13. Y. Gao, and K. Sorimachi, "Effect of manganese and titanium precipitates on the hot ductility of low carbon and ultra low carbon steels", *ISIJ Int. (Japan)*, Vol. 35, 1995, pp. 914-919.
14. L.E. Iorio, and W.M. Garrison, Jr., "Solubility of titanium carbosulfide in austenite", *ISIJ International (Japan)*, Vol. 42, 2002, pp. 545-550.

15. H. Shibata, T. Emi, and M. Suzuki, "In-situ real time observation of planar to cellular and cellular to dendritic transition of crystals growing in Fe-C alloy melts", *Materials Transactions, JIM*, Vol. 37, 1996, pp. 620-626.
16. N. Yuki, H. Shibata, and T. Emi, "Solubility of MnS in Fe-Ni alloys as determined by in situ observation of precipitation of MnS with a confocal scanning laser microscope", *ISIJ International (Japan)*, Vol. 38, 1998, pp. 317-323.
17. S. Kimura, K. Nakajima, S. Mizoguchi, and H. Hasegawa, "In-situ observation of the precipitation of manganese sulfide in low-carbon magnesium-killed steel", *Metallurgical and Materials Transactions A (USA)*, Vol. 33A, 2002, pp. 427-436.
18. M.C. Fleming, and T.K. Koseki, *Solidification of steel (chapter 6)*, in *The making, shaping and treating of steel (continuous casting)*, A.W. Cramb, Editor. 2003, The AISE Steel Foundation, Pittsburgh, PA.
19. M. Reid, D. Phelan, and R. Dippenaar, "Concentric Solidification for High Temperature Laser Scanning Confocal Microscopy", *ISIJ Int.*, Vol. 44, 2004, pp. 565-572.
20. Y. Ouchi, K. Oikawa, I. Ohnuma, and K. Ishida, "Effect of additional elements on the morphology of TiS in steels during solidification", *Materials Science Forum*, Vol. 284-286, 1998, pp. 509-515.